

Published in final edited form as:

*J Periodontol.* 2004 March ; 75(3): 429–440.

## Effect of Sustained Gene Delivery of Platelet-Derived Growth Factor or Its Antagonist (PDGF-1308) on Tissue-Engineered Cementum

Orasa Anusaksathien<sup>\*</sup>, Qiming Jin<sup>\*</sup>, Ming Zhao<sup>\*</sup>, Martha J. Somerman<sup>†</sup>, and William V. Giannobile<sup>\*,‡</sup>

<sup>\*</sup>Center for Craniofacial Regeneration and Department of Periodontics/Prevention/Geriatrics, School of Dentistry, University of Michigan, Ann Arbor, MI

<sup>†</sup>Currently, Department of Periodontics, University of Washington School of Dentistry, Seattle, WA; previously, Center for Craniofacial Regeneration and Department of Periodontics/Prevention/Geriatrics, School of Dentistry, University of Michigan

<sup>‡</sup>Department of Biomedical Engineering, College of Engineering, University of Michigan

### Abstract

**Background**—Cementum, a mineralized tissue lining the tooth root surface, is destroyed during the inflammatory process of periodontitis. Restoration of functional cementum is considered a criterion for successful regeneration of periodontal tissues, including formation of periodontal ligament, cementum, and alveolar bone. Short-term administration of platelet-derived growth factor (PDGF) has been shown to partially regenerate periodontal structures. Nonetheless, the role of PDGF in cementogenesis is not well understood. The aim of the present study was to determine the effect of sustained PDGF gene transfer on cementum formation in an ex vivo ectopic biomineralization model.

**Methods**—Osteocalcin (OC) promoter-driven SV40 transgenic mice were used to obtain immortalized cementoblasts (OCCM). The OCCM cells were transduced with adenoviruses (Ad) encoding either PDGF-A, an antagonist of PDGF signaling (PDGF-1308), a control virus (green fluorescent protein, GFP), or no treatment (NT). The transduced cells were incorporated into polymer scaffolds and implanted subcutaneously into severe combined immunodeficient (SCID) mice. The implants were harvested at 3 and 6 weeks for histomorphometric analysis of the newly formed mineralized tissues. Northern blot analysis was performed to determine the expression levels of mineral-associated genes including bone sialoprotein (BSP), OC, and osteopontin (OPN) in the cell-implant specimens at 3 and 6 weeks.

**Results**—The results indicated mineralization was significantly reduced in both the Ad/PDGF-A and Ad/PDGF-1308 treated specimens when compared to the NT or Ad/GFP groups at 3 and 6 weeks ( $P < 0.01$ ). In addition, the size of the implants treated with Ad/PDGF-A and Ad/PDGF-1308 was significantly reduced compared to implants from Ad/GFP and NT groups at 3 weeks ( $P < 0.05$ ). At 6 weeks, the size of implants and mineral formation increased in NT, Ad/GFP, and Ad/PDGF-A groups, while the Ad/PDGF-1308 treated implants continued to decrease in size and mineral formation ( $P < 0.01$ ). Northern blot analysis revealed that in the Ad/PDGF-A treated implants OPN was increased, whereas OC gene expression was downregulated at 3 weeks. In the Ad/PDGF-1308 treated implants, BSP, OC, and OPN were all downregulated at 3 weeks. At 3 weeks, the Ad/PDGF-

A treated implants contained significantly higher multinucleated giant cell (MNGC) density compared to NT, Ad/GFP, and Ad/PDGF-1308 specimens. The MNGC density in NT, Ad/GFP, and Ad/PDGF-A treated groups reduced over time, while the Ad/PDGF-1308 transduced implants continued to exhibit significantly higher MNGC density compared with the other treatment groups at 6 weeks.

**Conclusions**—The results showed that continuous exposure to PDGF-A had an inhibitory effect on cementogenesis, possibly via the upregulation of OPN and subsequent enhancement of MNGCs at 3 weeks. On the other hand, Ad/PDGF-1308 inhibited mineralization of tissue-engineered cementum possibly due to the observed downregulation of BSP and OC and a persistence of stimulation of MNGCs. These findings suggest that continuous exogenous delivery of PDGF-A may delay mineral formation induced by cementoblasts, while PDGF is clearly required for mineral neogenesis.

## Keywords

Cementogenesis; dental cementum; growth factors; platelet-derived; protein; green fluorescent

Periodontitis is a major cause of tooth loss in adults. The disease is characterized by the destruction of periodontal tissues including periodontal ligament, cementum (a mineralized tissue lining the tooth root surface), and alveolar bone. Proper formation of cementum is required for development of a functional periodontal ligament. Furthermore, the presence of healthy cementum is considered to be an important criterion for predictable restoration of periodontal tissues.<sup>1</sup> However, the mechanisms controlling development and regeneration of this tissue are not well understood. Platelet-derived growth factor (PDGF) has been shown to be involved in tooth development and cementogenesis.<sup>2,3</sup> The ability to provide sustained delivery of PDGF via gene transfer allows for the study of mechanisms controlling cementogenesis.

PDGF is an important stimulator of cellular chemotaxis, proliferation, and matrix synthesis.<sup>4-6</sup> It also exhibits anti-apoptosis activity.<sup>7</sup> The biological activities of PDGF are mediated through two intrinsic phosphotyrosine kinase receptors (PDGF $\alpha$ R and PDGF $\beta$ R) that induce several sets of signaling molecules.<sup>8</sup> Application of PDGF alone or in combination with insulin-like growth factor results in partial regeneration of periodontal tissues in preclinical and clinical investigations.<sup>9-12</sup> Results from studies using recombinant growth factors (GFs) to promote periodontal wound healing have not been as successful as hoped and have revealed limitations in time of exposure and bioavailability.<sup>13</sup> In order to prolong GF activity, gene therapy has been evaluated in several wound healing situations, including models associated with skin, bone, and periodontal tissues.<sup>14-16</sup> Our group previously reported that the application of adenovirus encoding PDGF (Ad/PDGF) to cells derived from the periodontium stimulates mitogenesis and proliferation of multiple cell types in vitro.<sup>17,18</sup> Using this approach, expression of PDGF was prolonged at both RNA and protein levels for at least a week. In addition, Ad/PDGF gene transfer resulted in sustained tyrosine kinase phosphorylation and downregulation of the growth arrest specific (*gas*) gene product PDGF $\alpha$ R for at least 96 hours.<sup>19</sup> Delivery of PDGF-B transgenes to human gingival fibroblasts stimulated cell proliferation, migration, and defect fill in an ex vivo three-dimensional wound model.<sup>20</sup> Most recently, in vivo gene transfer of Ad/PDGF-B was shown to stimulate periodontal tissue repair.<sup>21</sup>

Biodegradable polymers have great potential for the use in delivery of GFs to wound healing sites.<sup>22,23</sup> Three-dimensional polymer scaffolds provide a suitable environment for osteogenic cell proliferation and differentiation.<sup>24,25</sup> A gas foaming/particulate leaching approach has been implemented to fabricate porous (>95%) scaffolds from synthetic copolymers of lactide and glycolide (PLGA)<sup>26</sup> and has been used to successfully regenerate

bone and periodontal tissues.<sup>25,27,28</sup> Cementoblasts seeded in PLGA scaffolds under either static or dynamic conditions in vitro and implanted into SCID mice subcutaneously exhibit mineral formation.<sup>29</sup> Furthermore, transplantation of cementoblasts in PLGA scaffolds to periodontal fenestration defects promotes tissue repair.<sup>30</sup>

The establishment of a cementoblast cell line<sup>31</sup> enables us to study the effect of PDGF gene transfer on cementoblasts in vivo. The purpose of this study was to test the biological effects of ex vivo gene transfer of PDGF-A or an antagonist (PDGF-1308) on the formation of cementum in an ectopic biomineralization model in SCID mice. Also, the expression of mineral associated genes were determined. Results from these investigations will enhance our knowledge of the mechanisms controlling development, maintenance, and regeneration of cementum.

## MATERIALS AND METHODS

### Construction of Recombinant Adenoviruses

The construction of adenoviruses (Ad2 driven by the cytomegalovirus promoter [CMV]) encoding PDGF-A (Ad/PDGF-A) and its dominant negative mutant (Ad/PDGF-1308) has been previously described.<sup>17</sup> Briefly, the full-length murine PDGF-A or PDGF-1308 cDNA (kind gifts of Dr. C.D. Stiles, Boston, Massachusetts) was subcloned into a shuttle plasmid pAD2/CMV/SVIX<sup>§</sup> under the control of CMV promoter. Recombinant viral plaques were identified, selected, and purified. Titers of the viral stocks were determined on 293 cells by plaque assay and expressed as the number of plaque forming units (pfu) per ml.

### Cell Culture

The establishment of an immortalized murine cementoblast (OCCM) cell line has been reported in detail previously by D'Errico et al.<sup>31</sup> The OCCM cell line was maintained in Dulbecco's modified Eagle medium (DMEM),<sup>¶</sup> supplemented with 10% fetal calf serum<sup>¶</sup> (FCS), L-glutamine (2 mM), and antibiotics (100 units/ml penicillin and 100 µg/ml streptomycin<sup>¶</sup>) in a humidified atmosphere of 5% CO<sub>2</sub> in air at 37°C.

### Polymer Scaffold Fabrication

Poly (DL-lactic-co-glycolic acid; PLGA) three-dimensional scaffolds were processed into porous foams by an established solvent-casting, particulate-leaching technique as described previously.<sup>32,33</sup> These composites were cut into 5 × 5 × 2 mm blocks, sterilized with UV light, and stored until used. The resultant PLGA blocks were porous scaffolds containing 95% porosity and pore sizes ranging from 250 to 425 µm (Fig. 1A).

### Ex Vivo Transduction of OCCM Cells by PDGF-A or PDGF-1308 Transgenes and Implantation

OCCM cells (passage #16) were plated at 1 × 10<sup>6</sup> cells/plate and grown to confluence for 3 days (8 × 10<sup>6</sup> cells/plate). The expression of mineral-related genes including bone sialoprotein (BSP) and OC was confirmed by Northern blot analysis before use in each experiment. The cells were transduced with 100 MOI of Ad/PDGF-A, Ad/PDGF-1308, Ad/GFP, or no treatment (NT) in serum-free conditioned medium. After incubation and shaking every hour for 5 hours, the medium was replenished with DMEM supplemented with 10% FCS and further incubated overnight at 37°C. The adenoviral-treated or non-treated cells were incorporated into the PLGA scaffolds at 1 × 10<sup>6</sup> cells/sponge and cells allowed to attach to the polymer by incubation overnight at 37°C. The cell incorporated polymers were then implanted subcutaneously in

<sup>§</sup>Genzyme Corp., Cambridge, MA.

<sup>¶</sup>Gibco BRL Life Technologies, Inc., Grand Island, NY.

<sup>¶</sup>Gemini Bio-Products, Woodland, CA.

immunodeficient (SCID) mice (Fig. 1B). The surgical procedure has been described previously in detail by Jin et al.<sup>29</sup> The management of the animals was performed in accordance with a protocol approved by the Committee on the Care and Use of Animals at the University of Michigan. Four blocks of cell-implants were placed in the dorsum of each animal. Assessments included histological evaluation (n = 3 implants/group) and RNA analysis by reverse transcription polymerase chain reaction (RT-PCR) and Northern blot (n = 3 implants/group). The implants were harvested at 3 and 6 weeks and fixed in Bouin's solution (0.9% picric acid, 9% vol/vol formaldehyde, and 5% acetic acid).<sup>#</sup> The specimens were then decalcified with 10% vol/vol acetic acid, 4% vol/vol formaldehyde, 0.85% NaCl for 2 to 3 weeks, cut in the center, and embedded in paraffin. The specimens were sectioned at 5  $\mu$ m and stained with hematoxylin and eosin (H&E).

### RNA Extraction from Polymer-Cell Implants

For RNA analyses, after removal of implants, specimens were immediately snap frozen using liquid nitrogen. Each specimen was ground into small pieces and transferred to an Eppendorf tube. The tissue pellet was precipitated by adding 1 ml of Trizol,<sup>||</sup> vortexed for 30 minutes at room temperature, and centrifuged at 10,000 rpm for 10 minutes at 4°C. The supernatant was collected and total RNA was extracted for evaluation by RT-PCR or Northern blot analysis (see below).

### Sustained Expression of PDGF Genes In Vivo Using RT-PCR

Reverse transcription polymerase chain reaction was performed to determine the prolonged expression of PDGF genes by adenovirus infection in vivo. One  $\mu$ g of total RNA extracted from PLGA-cell implants at 3 and 6 weeks was reverse transcribed using a kit.<sup>\*\*</sup> A primer pair was specifically designed to determine the expression of Ad/PDGF-A and Ad/PDGF-1308. The forward primer located at the 3' end of the PDGF-A or PDGF-1308 gene was 5'-TCGCAGGAAGAGAAGTATTG-3'. The reverse primer included the adenovirus backbone for both constructs was 5'-CATCAATGTATCTTATCACGCG-3'. Endogenous PDGF-A expression was also performed using a primer pair 5'-CCTGTGCCCCATTCGCAGGAAGAG-3' and 5'-TTGGCCACCTTGACACTGCG-3'. The housekeeping gene,  $\beta$ -actin, was used to assess the loading of the samples. A total of 25  $\mu$ l of PCR reaction was mixed with 5  $\mu$ l of RT product, PCR buffer (10 mM Tris-HCl, pH 9.0, 50 mM KCl, and 0.1% Triton X-100), 0.2 mM dNTPs, 2.5 mM MgCl<sub>2</sub>, 20 pM of each primer, 0.5 unit of Taq DNA polymerase<sup>††</sup> using a thermocycler 9600.<sup>‡‡</sup> The PCR conditions for detecting the expression of adenoviruses encoding PDGF-A and PDGF-1308 were 94°C for 2 minutes, 35 cycles of 94°C for 30 seconds, 60°C for 30 seconds, followed by 72°C for 45 seconds. PCR conditions for detection of endogenous PDGF-A and  $\beta$ -actin were the same, except only 30 cycles were performed. The expected PCR product was 638 bp for both Ad/PDGF-A and Ad/PDGF-1308, 226 bp for endogenous PDGF-A, and 248 bp for  $\beta$ -actin.

### Histomorphometry

Histomorphometric analysis was used to determine the size dimensions of the implants from the gross specimens at 3 and 6 weeks using a computer-assisted image analysis program. The size of the implants, the total area of mineralization, and density of formed mineral were evaluated from standardized images captured from the 3- and 6-week H&E-stained sections at 20  $\times$  magnification. A single masked calibrated examiner (OA) evaluated the size of the specimens and areas of mineralization using a software program<sup>§§</sup> and demonstrated a pre-

<sup>#</sup>Polysciences, Warrington, PA.

<sup>\*\*</sup>Retroscrip, Ambion, Inc., Austin, TX.

<sup>††</sup>Promega Co., Madison, WI.

<sup>‡‡</sup>Perkin Elmer, Norwalk, CT.

and post-study calibration intraexaminer error of <5%. Because the implants were sectioned in half at the center of the specimen before paraffin embedding, the total area of specimen was determined two-dimensionally by drawing a perimeter line along a representative section of each implant. Percentage of mineral to total tissue (density) of the implants was determined by dividing area of mineralization by total area of the specimen as previously described.<sup>29</sup> In addition, the number of multinucleated giant cells (MNGCs) was counted in each specimen at 3 and 6 weeks. Cell density was determined by dividing cell number by the total tissue area for each specimen. The specimens were uncoded and mean and standard error measurements were calculated for each treatment group. One-way analysis of variance (ANOVA) and Tukey multiple comparison tests were utilized to evaluate the difference in the size of the specimens, area of mineralization, mineral density, and MNGC density between groups.

### Northern Blot Analysis

To determine the expression of genes regulated by PDGF in vivo, Northern blot analysis was performed. Ten µg of total RNA was denatured, separated in a 6% formaldehyde/1.2% agarose gels, transferred onto a nylon membrane,<sup>¶¶¶</sup> and immobilized. Probes used for Northern blot analysis included murine OC cloned into pSP65<sup>34</sup> (a gift of Dr. J. Wozney, Genetic Institute, Boston, Massachusetts), 1 kb PCR product of BSP, and osteopontin (OPN) cloned into PCR II vector (gifts of Drs. M. Young and L. Fisher NIDCR/NIH, Bethesda, Maryland).<sup>35,36</sup> The blots were then hybridized with <sup>32</sup>P-labeled probes generated from randomly primed cDNA<sup>¶¶¶</sup> and exposed to films with intensifying screens at -70°C for 6 to 24 hours. An 18S RNA probe was used to evaluate the relative loading of RNA samples.

### Cell Survival Analysis

To determine the ability of Ad/PDGF-A or Ad/PDGF-1308 gene transfer to induce apoptosis in OCCM cells, caspase 3/7 activities were assayed using a caspase 3/7 kit.<sup>††</sup> OCCM cells were plated at  $2 \times 10^4$  cell/well in a 96 well plate and incubated O/N at 37°C. The protocol for adenovirus transduction with 10 and 100 MOI of Ad/PDGF-A or Ad/PDGF-1308 was similar to that described above. However, the use of Ad/GFP interfered with fluorescent wavelength in the system, therefore Ad/luciferase (adenovirus encoding luciferase driven by the CMV promoter; kind gift of Selective Genetics, Inc., San Diego, California) was utilized in these experiments. Induction of apoptosis in OCCM cells by treatment with 100 µM of the chemotherapeutic agent, etoposide, for 16 hours was used as a positive control. Each experiment was performed in duplicate. Caspase 3/7 activities were assayed following the manufacturer's protocol 24 and 48 hours following Ad/PDGF-A or Ad/PDGF-1308 gene transfer or 20 ng/ml of rhPDGF-AA<sup>###</sup> application. In addition, terminal deoxynucleotidyl transferase-mediated dUTP nick-end labeling (TUNEL) staining was performed on 3- and 6-week specimens to determine induction of apoptosis in tissue specimens following gene transfer of PDGF-A or PDGF-1308.

## RESULTS

### Sustained Expression of PDGF Genes in OCCM-PLGA Implants

Images depicting the microscopic structure of PLGA scaffold-OCCM implants transduced by Ad/GFP for 48 hours are presented in Figure 1A. An open pore structure of the PLGA scaffolds allowed for penetration and adherence by the transduced cells as shown by phase contrast and fluorescence microscopy. Having established that these scaffolds provide a positive

§§Image Pro Plus, Media Cybernetics, Silver Spring, MD.

¶¶¶Duralon, Stratagene, Inc., La Jolla, CA.

¶¶¶Rediprime, Amersham, Arlington Heights, IL.

###Upstate Biotechnology, Lake Placid, NY.

environment for cells transduced by adenoviruses, the cells were combined with PLGA and implanted in SCID mice. Implant specimens retrieved at 3 and 6 weeks demonstrated prolonged expression of Ad/PDGF-A and Ad/PDGF-1308 as analyzed by RT-PCR (Fig. 2). No such expression was detectable in the NT and Ad/GFP groups. Endogenous PDGF-A expression was detected at similar levels in all OCCM-implant groups for up to 6 weeks (Fig. 2).

### Descriptive Histology

The gross appearance of the implants and measurements of the implant sizes at 3 and 6 weeks are shown in Figures 3A and 3B. Significantly smaller implant dimensions were observed for the Ad/PDGF-A and Ad/PDGF-1308 treated specimens compared with NT and Ad/GFP implants at 3 weeks ( $P < 0.05$ ). All of the implants increased in size from 3 to 6 weeks, except for the Ad/PDGF-1308 treated implants which were significantly smaller when compared with NT or Ad/GFP groups by 6 weeks ( $P < 0.01$ ).

The histological appearance of implants retrieved from SCID mice is shown in Figure 4. Significant evidence of immature mineral formation (woven-like appearance) was detected in the NT and Ad/GFP groups at 3 weeks, with increased mineral formation 6 weeks post-implantation. Minimal to no mineral formation was detected in both the Ad/PDGF-A ( $n = 2/3$ ) and Ad/PDGF-1308 ( $n = 3/3$ ) treated implants at 3 weeks, but by 6 weeks there was evidence of mineral neogenesis. The Ad/PDGF-A treated implants exhibited mature mineral formation at 6 weeks, while Ad/PDGF-1308 specimens revealed a paucity of mineral (Fig. 4).

Multinucleated giant cell infiltration was present along the lattices in all the samples at 3 weeks (Fig. 5A). Cell density analyses revealed that Ad/PDGF-A and Ad/PDGF-1308 treated groups contained significantly higher MNGC density versus both control groups at 3 weeks ( $P < 0.001$ , Fig. 5B), and the Ad/PDGF-A treated implants exhibited greater MNGC density versus the Ad/PDGF-1308 group at this time point ( $P < 0.05$ ). At 6 weeks, the number of MNGCs in the Ad/PDGF-A treated implants decreased and was comparable to NT and Ad/GFP specimens; however, the Ad/PDGF-1308 treated implants showed continued elevation of MNGC density when compared with the other treatment groups ( $P < 0.05$ ).

### Histomorphometry

Histomorphometric analyses of the total area of mineralization, and mineral density at 3 and 6 weeks post-implantation are shown in Figure 6. The total area of mineralization was significantly less in the Ad/PDGF-A and Ad/PDGF-1308 groups compared to NT and Ad/GFP specimens at both 3 weeks ( $P < 0.001$ ) and 6 weeks ( $P < 0.05$ ; Fig. 6A). The mineral density of the Ad/PDGF-A group was significantly less than the control groups at 3 weeks ( $P < 0.01$ ), while at 6 weeks mineral density was similar to controls (Fig. 6B). Ad/PDGF-1308 treatment resulted in significantly reduced mineralization that was sustained for the 6-week observation period ( $P < 0.05$ ; Fig. 6B).

### Expression of Mineral-Associated Genes in Cementoblasts in Response to PDGF Gene Transfer

To determine the effect of PDGF-A and PDGF-1308 on the modulation of cementum neogenesis in vivo, the expression of genes associated with mineral formation, including BSP, OC, and OPN, were evaluated in implants retrieved at 3 and 6 weeks using Northern blot analysis (Fig. 7). The levels of gene expression were normalized to 18S RNA to compensate for loading of RNA. At 3 weeks, BSP expression levels were similar in NT, Ad/GFP, and Ad/PDGF-A groups, while RNA from Ad/PDGF-1308 treated implants lacked transcription for BSP. Expression of OC was downregulated in implants from Ad/GFP and Ad/PDGF-A when compared to implants from NT, whereas no detectable level of OC mRNA was observed in the Ad/PDGF-1308 implants at 3 weeks. Ad/PDGF-A exposure upregulated the expression

of OPN, while Ad/PDGF-1308 reduced OPN gene expression at 3 weeks. By 6 weeks, gene expression of BSP, OC, and OPN was relatively similar in samples from all groups.

### OCCM Cell Apoptosis

PDGF has been reported to be a cell survival factor.<sup>7</sup> Therefore, we sought to determine whether any of the results observed were due to Ad/PDGF-A or Ad/PDGF-1308 mediated OCCM cell death. Apoptosis was evaluated in vitro using caspase 3/7 activities and in tissue samples using TUNEL staining. The caspase 3/7 assay was performed at 24 and 48 hours following transduction of OCCM cells with 10 and 100 MOI of Ad/Luc, Ad/PDGF-A, Ad/PDGF-1308, 20 ng/ml rhPDGF-AA, or NT. The levels of caspase 3/7 activities were not significantly different among any of the treatment groups at any time point for both doses of adenovirus as compared to the NT control (data not shown). However, all groups exhibited decreased caspase 3/7 activities compared to etoposide treatment (positive control). In addition, no difference in TUNEL staining was noted among any of the groups (data not shown).

### DISCUSSION

Several animal models indicate that bolus delivery of PDGF results in significant regeneration of new cementum, periodontal ligament, and alveolar bone.<sup>9-11</sup> To our knowledge, this is the first in vivo study directed toward determining the long-term effect of PDGF on cementum formation. In the present study, the long-term effect of PDGF-A gene delivery on cementum formation was examined using three-dimensional scaffolds implanted in vivo. The reduction of implant size in the Ad/PDGF-A treated implants at 3 weeks was unexpected since cementoblasts exposed to either Ad/PDGF-A or PDGF-AA protein in vitro exhibited enhanced proliferation versus untreated cells.<sup>18</sup> One possible explanation for this apparent discrepancy in implant size may be related to the large number of MNGCs associated with the Ad/PDGF-A treated implants (Fig. 5A). Platelet-derived growth factor is a potent chemotactic factor for macrophages.<sup>37</sup> Also, high levels of PDGF gene expression have been detected in macrophages that infiltrate soft tissues surrounding failing implants derived from patients receiving total hip replacement.<sup>38</sup> Similarly, Salcetti et al. reported elevations of PDGF in gingival crevicular fluid obtained from failing dental implants as compared to healthy osseointegrated fixtures.<sup>39</sup> Furthermore, significantly higher levels of PDGF were detected in tissue derived from chronic periodontitis lesions compared to healthy sites.<sup>40</sup> Platelet-derived growth factor has been shown to stimulate osteoclastic bone resorption directly.<sup>41</sup> In addition, PDGF secreted by osteoclasts was reported to inhibit osteoblastic differentiation.<sup>42</sup> Therefore, the presence of MNGCs in the Ad/PDGF-A treated implants may have had a negative effect on cementoblast differentiation and matrix formation.

Histomorphometric analysis showed that mineralization was reduced at 3 weeks in the Ad/PDGF-A treated implants as compared to NT and Ad/GFP groups. In support of this finding, continuous exposure to PDGF inhibited both osteoblast- and cementoblast-mediated mineral nodule formation in vitro and in these in vitro studies this was attributed to increased proliferation, followed by decreased cell differentiation.<sup>43,44</sup> However, exposure of cementoblasts to PDGF for 24 or 72 hours in vitro prior to implantation did not block mineral formation in implants retrieved at 6 weeks<sup>43</sup> and in osteoblasts in vitro pulse treated with PDGF, mineral nodule formation was enhanced.<sup>44</sup> Short-term treatment with PDGF stimulated DNA synthesis in osteoblasts without inhibiting differentiating function of osteoblasts, whereas continuous application of PDGF blocked osteoblast differentiation in vitro.<sup>44</sup> Ad/PDGF-A treated implants exhibited mineral neogenesis at 6 weeks, albeit at lower levels than NT (Fig. 6). Results from previous studies<sup>42,44</sup> and those reported here suggest that brief exposure of cementoblasts to PDGF might enhance formation of mineral, while continuous exposure is inhibitory by blocking cementoblast differentiation in vivo. Further

studies are required to determine the mechanism(s) controlling PDGF regulation of mineralization in vivo and, furthermore, if this is related to biphasic responses or decreased levels of PDGF expressed at 6 weeks in this model.

Northern analysis of genes associated with mineral formation showed that OPN was increased in Ad/PDGF-A treated implants at 3 weeks, while OC was slightly downregulated compared with NT and Ad/GFP groups (Fig. 7). At 6 weeks, the levels of OPN, BSP, and OC expression in the Ad/PDGF-A treated implants were similar to the other three groups. These results parallel our in vitro studies where we reported that application of PDGF-AA or PDGF gene transfer to cementoblasts resulted in up-regulation of OPN and a reduction of BSP and OC gene expression.<sup>18,43</sup> Existing data support the role for OPN as a regulator of matrix mineralization. Bones from OPN-deficient mice exhibit an increased mineral content and crystal size.<sup>45</sup> Interestingly, OPN has been reported to promote macrophage migration, attachment, and function.<sup>46</sup> In this regard, the increase in the number of MNGCs associated with the PLGA scaffolds in the Ad/PDGF-A treated group compared to the other groups may be related to the direct effect of PDGF as discussed above, as well as PDGF-mediated induction of high OPN levels (Figs. 5A and B). Therefore, inhibition of mineral neogenesis in Ad/PDGF-A treated implants at 3 weeks might be mediated through the upregulation of the OPN gene. Collectively, high levels of PDGF produced during the first 3 weeks of implantation and induction of OPN expression by PDGF are likely to be responsible for the recruitment of MNGCs, mimicking chronic inflammation.<sup>47</sup> This, in turn, inhibited cementoblast differentiation as evidenced by decreased expression of OC, a marker of cementoblast differentiation and subsequently limited biomineralization. By 6 weeks, PDGF production appeared to be reduced and expression of genes associated with mineral formation were similar to those of untreated samples, thus allowing for mineral formation.

The mechanisms by which PDGF controls the expression of BSP and OC genes in cementoblasts are not well characterized. One of the possible explanations is that PDGF directly or indirectly exerts its effects on BSP and OC gene expression via up-regulation of transforming growth factor (TGF)- $\beta$ .<sup>37,48</sup> TGF- $\beta$ 's effects on BSP and OC gene expression in cementoblasts and osteoblasts are similar to those of PDGF; however, TGF- $\beta$  did not promote cementoblast proliferation in vitro.<sup>43,49</sup> It has been shown that the rat BSP promoter contains a TGF- $\beta$  activation element that is involved in induction of BSP in response to TGF- $\beta$ .<sup>50</sup> After triggering of receptor phosphorylation, PDGF transduces signals from the cell surface to the nucleus by activating the extracellular signal-regulated kinase (ERK) via the Ras/Raf/MEK/ERK cascade in osteoblasts.<sup>51</sup> It has been shown that TGF- $\beta$  suppresses OC gene expression via the ERK pathway in the human osteoblast culture system.<sup>52</sup> We have also shown that application of Ad/PDGF-A resulted in sustained phosphorylation of PDGF $\alpha$ R as well as prolonged phosphorylation of the downstream ERK1/2 signaling pathway.<sup>19</sup> Therefore, it is possible that down regulation of OC expression by PDGF gene transfer is mediated via ERK signaling in cementoblasts. The signaling mechanisms involved in PDGF regulation on genes associated with matrix protein expression await further studies.

PDGF-1308 is a dominant negative mutant that possesses antagonistic effects through formation of inactive and unstable heterodimers with wild type PDGF-A or-B chains.<sup>53</sup> The biological activities of PDGF are exerted through the autophosphorylation of its tyrosine kinase receptor dimerization.<sup>8</sup> It has been shown that Ad/PDGF-1308 completely abolishes the activated state of PDGF $\alpha$ R by blocking phosphorylation of the receptor that disrupts PDGF bio-activity.<sup>19</sup> In addition, cells transduced with PDGF-1308 exhibit a decrease in cell proliferation.<sup>54</sup> In the present study, the implant size in the Ad/PDGF-1308 treated implants continued to decrease even at 6 weeks and was unrelated to apoptosis (as determined by TUNEL staining and caspase 3/7 activities). Therefore, continued reduction of implant size in the Ad/PDGF-1308 treated group may be mediated through the inhibition of OCCM



proliferation. Also, the growth inhibitory effect in the Ad/PDGF-1308 treated implants may be governed in part by the persistence of MNGCs during the 6-week observation period.

The mechanism involved in the inhibition of mineral formation mediated by Ad/PDGF-1308 clearly differed from that noted with Ad/PDGF-A treatment. The antagonistic activities of PDGF-1308 may not only inhibit cell proliferation, but also reduce matrix formation. Northern analysis showed that expression of BSP and OC were dramatically downregulated in the Ad/PDGF-1308 treated implants at 3 weeks. Evidence to date suggests that BSP is a nucleator of hydroxyapatite crystal formation,<sup>55,56</sup> while OC appears to play a role in early phases of mineralization and in regulation of crystal growth.<sup>56,57</sup> Thus, suppression of mineral formation in the Ad/PDGF-1308 treated implants at 3 weeks may be mediated by inhibition of BSP and OC expression. Also, elevated levels of MNGC density were observed in the Ad/PDGF-1308 treated implants as compared to the NT and Ad/GFP groups at 3 and 6 weeks (Fig. 5B). As stated above, PDGF is a potent chemotactic factor for macrophages.<sup>37</sup> Although OPN expression was slightly downregulated in the Ad/PDGF-1308 treated group, one possible explanation, while highly speculative, is that PDGF-1308 might recruit MNGCs into the scaffolds without the ability of the cells to recognize the difference in the amino acid change in the PDGF-1308 molecule. This may be one of the contributing factors that resulted in reduced mineralization induced by cementoblasts infected by Ad/PDGF-1308. These results suggest that endogenous PDGF plays an important role in cementoblast proliferation and differentiation, although there may be other direct or indirect functions of PDGF on cementoblast activity that remain to be determined.

Although it is difficult to measure the actual production of PDGF-AA protein in this in vivo model, we have shown prolonged expression of Ad/PDGF-A and Ad/PDGF-1308 genes up to 6 weeks by RT-PCR (Fig. 2). The results suggest that transduced OCCM cells were able to produce biologically active PDGF proteins. It has been estimated that cells transduced with Ad/PDGF-A produce ~200 ng of PDGF-AA per 10<sup>6</sup> cells per day.<sup>19</sup> This level of PDGF-AA production appears to be sufficient to exert biological effects on the surrounding host cells; e.g., MNGCs that infiltrate the cell-implants presumably through gradient diffusion of PDGF. Additional studies will be needed to elucidate the release characteristics of transduced cells by adenovirus in vivo. Furthermore, we acknowledge the limitations of this ectopic model for the generation of tissue-engineered cementum. The contribution of the tooth root surface cannot be underestimated in terms of the signaling mechanisms controlling cementogenesis. We have recently reported the behavior of these cloned cementoblasts in periodontal wounds.<sup>30</sup> Indeed, the tissue-engineered cementum forms mineral in the position of the supporting bone as well as early evidence of root-lining tissue neogenesis. Future studies will examine the ability of genetically-modified cementoblasts to promote periodontal tissue regeneration.

In summary, the effect of long-term delivery of PDGF-A and PDGF-1308 via gene transfer on cementum formation was examined in three-dimensional scaffolds implanted subcutaneously in vivo. PDGF-A appears to initially inhibit growth and biomineralization at 3 weeks, with recovery from these effects at 6 weeks. This result might be governed through the upregulation of OPN at 3 weeks and the dose of PDGF delivered by gene transfer. In contrast, the PDGF antagonist (PDGF-1308) inhibited cell growth and mineral formation for the entire 6-week study. This may be mediated by suppression of BSP and OC gene expression as well as inhibition of endogenous PDGF and persistent stimulation of MNGCs noted with OCCM-polymer implants. These findings suggest that continuous exogenous delivery of PDGF-A may delay mineral formation induced by cementoblasts, while PDGF is clearly required for mineral neogenesis.

## Acknowledgements

The authors thank Dr. Zhuoran Zhao, University of Michigan, Ann Arbor, Michigan, for performing some of the histomorphometric analysis. We also thank Jan Berry, Sarah Webb, and Christopher Strayhorn, University of Michigan, for their technical assistance. We also appreciate the assistance of Chris Jung, University of Michigan, with the preparation of the figures. This study was supported by NIH/NIDCR grants DE 11960 (WVG), DE 13397 (WVG and MJS), DE 09532 (MJS and WVG), and DE 13047 (MJS).

## References

1. Saygin NE, Giannobile WV, Somerman MJ. Molecular and cell biology of cementum. *Periodontol* 2000;24:73–98. [PubMed: 11276875]
2. Lynch SE, de Castilla GR, Williams RC, et al. The effects of short-term application of a combination of platelet-derived and insulin-like growth factors on periodontal wound healing. *J Periodontol* 1991;62:458–467. [PubMed: 1920013]
3. Chai Y, Bringas P Jr, Mogharei A, Shuler CF, Slavkin HC. PDGF-A and PDGFR- $\alpha$  regulate tooth formation via autocrine mechanism during mandibular morphogenesis in vitro. *Dev Dyn* 1998;213:500–511. [PubMed: 9853970]
4. Kaplan DR, Chao FC, Stiles CD, Antoniades HN, Scher CD. Platelet alpha granules contain a growth factor for fibroblasts. *Blood* 1979;53:1043–1052. [PubMed: 444648]
5. Seppa H, Grotendorst G, Seppa S, Schiffmann E, Martin GR. Platelet-derived growth factor in chemotactic for fibroblasts. *J Cell Biol* 1982;92:584–588. [PubMed: 7061598]
6. Heldin P, Laurent TC, Heldin CH. Effect of growth factors on hyaluronan synthesis in cultured human fibroblasts. *Biochem J* 1989;258:919–922. [PubMed: 2543365]
7. Romashkova JA, Makarov SS. NF- $\kappa$ B is a target of AKT in anti-apoptotic PDGF signalling. *Nature* 1999;401:86–90. [PubMed: 10485711]
8. Heldin CH, Ostman A, Ronnstrand L. Signal transduction via platelet-derived growth factor receptors. *Biochim Biophys Acta* 1998;1378:F79–F113. [PubMed: 9739761]
9. Rutherford RB, Niekrash CE, Kennedy JE, Charette MF. Platelet-derived and insulin-like growth factors stimulate regeneration of periodontal attachment in monkeys. *J Periodontol Res* 1992;27:285–290. [PubMed: 1640350]
10. Giannobile WV, Finkelman RD, Lynch SE. Comparison of canine and non-human primate animal models for periodontal regenerative therapy: Results following a single administration of PDGF/IGF-I. *J Periodontol* 1994;65:1158–1168. [PubMed: 7877089]
11. Giannobile WV, Hernandez RA, Finkelman RD, et al. Comparative effects of platelet-derived growth factor-BB and insulin-like growth factor-I, individually and in combination, on periodontal regeneration in *Macaca fascicularis*. *J Periodontol Res* 1996;31:301–312. [PubMed: 8858534]
12. Howell TH, Fiorellini JP, Paquette DW, et al. A phase I/II clinical trial to evaluate a combination of recombinant human platelet-derived growth factor-BB and recombinant human insulin-like growth factor-I in patients with periodontal disease. *J Periodontol* 1997;68:1186–1193. [PubMed: 9444594]
13. Anusaksathien O, Giannobile WV. Growth factor delivery to re-engineer periodontal tissues. *Curr Pharm Biotechnol* 2002;3:129–139. [PubMed: 12022256]
14. Fang J, Zhu YY, Smiley E, et al. Stimulation of new bone formation by direct transfer of osteogenic plasmid genes. *Proc Natl Acad Sci (USA)* 1996;93:5753–5758. [PubMed: 8650165]
15. Eriksson E, Yao F, Svensjo T, et al. In vivo gene transfer to skin and wound by microseeding. *J Surg Res* 1998;78:85–91. [PubMed: 9733623]
16. Jin QM, Anusaksathien O, Webb SA, Rutherford RB, Giannobile WV. Gene therapy of bone morphogenetic protein for periodontal tissue engineering. *J Periodontol* 2003;74:202–213. [PubMed: 12666709]
17. Zhu Z, Lee CS, Tejada KM, Giannobile WV. Gene transfer and expression of platelet-derived growth factors modulate periodontal cellular activity. *J Dent Res* 2001;80:892–897. [PubMed: 11379891]
18. Giannobile WV, Lee CS, Tomala MP, Tejada KM, Zhu Z. Platelet-derived growth factor (PDGF) gene delivery for application in periodontal tissue engineering. *J Periodontol* 2001;72:815–823. [PubMed: 11453245]

19. Chen Q-P, Giannobile WV. Adenoviral gene transfer of PDGF downregulates *gas* gene product PDGF $\alpha$ R and prolongs ERK and Akt/PKB activation. *Am J Physiol Cell Physiol* 2002;282:C538–544. [PubMed: 11832339]
20. Anusaksathien O, Webb SA, Jin Q-M, Giannobile WV. PDGF gene delivery stimulates *ex vivo* gingival wound repair. *Tissue Eng* 2003;9:745–756. [PubMed: 13678451]
21. Jin QM, Anusaksathien O, Webb SA, Printz MA, Giannobile WV. Engineering of tooth-supporting structures by delivery of PDGF gene therapy vectors. *Mol Ther*. 2004in press
22. Richardson TP, Peters MC, Ennett AB, Mooney DJ. Polymeric system for dual growth factor delivery. *Nat Biotechnol* 2001;19:1029–1034. [PubMed: 11689847]
23. Yang XB, Roach HI, Clarke NM, et al. Human osteoprogenitor growth and differentiation on synthetic biodegradable structures after surface modification. *Bone* 2001;29:523–531. [PubMed: 11728922]
24. Ishaug SL, Crane GM, Miller MJ, et al. Bone formation by three-dimensional stromal osteoblast culture in biodegradable polymer scaffolds. *J Biomed Mater Res* 1997;36:17–28. [PubMed: 9212385]
25. Shea LD, Wang D, Franceschi RT, Mooney DJ. Engineered bone development from a pre-osteoblast cell line on three-dimensional scaffolds. *Tissue Eng* 2000;6:605–617. [PubMed: 11103082]
26. Harris LD, Kim BS, Mooney DJ. Open pore biodegradable matrices formed with gas foaming. *J Biomed Mater Res* 1998;42:396–402. [PubMed: 9788501]
27. Mattson JS, Gallagher SJ, Jabro MH. The use of 2 bioabsorbable barrier membranes in the treatment of interproximal intrabony periodontal defects. *J Periodontol* 1999;70:510–517. [PubMed: 10368055]
28. Sigurdsson TJ, Nygaard L, Tatakis DN, et al. Periodontal repair in dogs: Evaluation of rhBMP-2 carriers. *Int J Periodontics Restorative Dent* 1996;16:524–537. [PubMed: 9242091]
29. Jin QM, Zhao M, Webb SA, et al. Cementum engineering using three-dimensional polymer scaffolds. *J Biomed Mater Res* 2003;67A:54–60.
30. Zhao M, Jin QM, Berry JE, Nociti FH Jr, Giannobile WV, Somerman MJ. Cementoblast delivery for periodontal tissue engineering. *J Periodontol* 2004;75:154–161. [PubMed: 15025227]
31. D'Errico JA, Ouyang H, Berry JE, et al. Immortalized cementoblasts and periodontal ligament cells in culture. *Bone* 1999;25:39–47. [PubMed: 10423020]
32. Mooney DJ, Sano K, Kaufmann PM, et al. Long-term engraftment of hepatocytes transplanted on biodegradable polymer sponges. *J Biomed Mater Res* 1997;37:413–420. [PubMed: 9368146]
33. Murphy WL, Dennis RG, Kileny JL, Mooney DJ. Salt fusion: An approach to improve pore interconnectivity within tissue engineering scaffolds. *Tissue Eng* 2002;8:43–52. [PubMed: 11886653]
34. Wozney JM. The bone morphogenetic protein family and osteogenesis. *Mol Reprod Dev* 1992;32:160–167. [PubMed: 1637554]
35. Young MF, Kerr JM, Termine JD, et al. cDNA cloning, mRNA distribution and heterogeneity, chromosomal location, and RFLP analysis of human osteopontin (OPN). *Genomics* 1990;7:491–502. [PubMed: 1974876]
36. Young MF, Ibaraki K, Kerr JM, Lyu MS, Kozak CA. Murine bone sialoprotein (BSP): cDNA cloning, mRNA expression, and genetic mapping. *Mamm Genome* 1994;5:108–111. [PubMed: 8180469]
37. Pierce GF, Mustoe TA, Lingelbach J, et al. Platelet-derived growth factor and transforming growth factor-beta enhance tissue repair activities by unique mechanisms. *J Cell Biol* 1989;109:429–440. [PubMed: 2745556]
38. Jiranek WA, Machado M, Jasty M, et al. Production of cytokines around loosened cemented acetabular components. Analysis with immunohistochemical techniques and in situ hybridization. *J Bone Joint Surg Am* 1993;75:863–879. [PubMed: 8314826]
39. Salcetti JM, Moriarty JD, Cooper LF, et al. The clinical, microbial, and host response characteristics of the failing implant. *Int J Oral Maxillofac Implants* 1997;12:32–42. [PubMed: 9048452]
40. Pinheiro M-LB, Feres-Filho EJ, Graves DT, et al. Quantification and localization of platelet-derived growth factor in gingiva of periodontitis patients. *J Periodontol* 2003;74:323–328. [PubMed: 12710751]

41. Zhang Z, Chen J, Jin D. Platelet-derived growth factor (PDGF)-BB stimulates osteoclastic bone resorption directly: The role of receptor beta. *Biochem Biophys Res Commun* 1998;251:190–194. [PubMed: 9790928]
42. Kubota K, Sakikawa C, Katsumata M, Nakamura T, Wakabayashi K. Platelet-derived growth factor BB secreted from osteoclasts acts as an osteoblastogenesis inhibitory factor. *J Bone Miner Res* 2002;17:257–265. [PubMed: 11811556]
43. Saygin NE, Tokiyasu Y, Giannobile WV, Somerman MJ. Growth factors regulate expression of mineral associated genes in cementoblasts. *J Periodontol* 2000;71:1591–1600. [PubMed: 11063392]
44. Hsieh SC, Graves DT. Pulse application of platelet-derived growth factor enhances formation of a mineralizing matrix while continuous application is inhibitory. *J Cell Biochem* 1998;69:169–180. [PubMed: 9548564]
45. Boskey AL, Spevak L, Paschalis E, Doty SB, McKee MD. Osteopontin deficiency increases mineral content and mineral crystallinity in mouse bone. *Calcif Tissue Int* 2002;71:145–154. [PubMed: 12073157]
46. Giachelli CM, Steitz S. Osteopontin: A versatile regulator of inflammation and biomineralization. *Matrix Biol* 2000;19:615–622. [PubMed: 11102750]
47. Giachelli CM, Lombardi D, Johnson RJ, Murry CE, Almeida M. Evidence for a role of osteopontin in macrophage infiltration in response to pathological stimuli in vivo. *Am J Pathol* 1998;152:353–358. [PubMed: 9466560]
48. Pierce GF, Mustoe TA, Lingelbach J, et al. Transforming growth factor beta reverses the glucocorticoid-induced wound-healing deficit in rats: Possible regulation in macrophages by platelet-derived growth factor. *Proc Natl Acad Sci (USA)* 1989;86:2229–2233. [PubMed: 2928327]
49. Yu X, Hsieh SC, Bao W, Graves DT. Temporal expression of PDGF receptors and PDGF regulatory effects on osteoblastic cells in mineralizing cultures. *Am J Physiol* 1997;272:C1709–1716. [PubMed: 9176163]
50. Ogata Y, Niisato N, Furuyama S, et al. Transforming growth factor-beta 1 regulation of bone sialoprotein gene transcription: Identification of a TGF-beta activation element in the rat BSP gene promoter. *J Cell Biochem* 1997;65:501–512. [PubMed: 9178100]
51. Chaudhary LR, Avioli LV. Activation of extracellular signal-regulated kinases 1 and 2 (ERK1 and ERK2) by FGF-2 and PDGF-BB in normal human osteoblastic and bone marrow stromal cells: Differences in mobility and in-gel renaturation of ERK1 in human, rat, and mouse osteoblastic cells. *Biochem Biophys Res Commun* 1997;238:134–139. [PubMed: 9299466]
52. Lai CF, Cheng SL. Signal transductions induced by bone morphogenetic protein-2 and transforming growth factor-beta in normal human osteoblastic cells. *J Biol Chem* 2002;277:15514–15522. [PubMed: 11854297]
53. Mercola M, Deininger PL, Shamah SM, et al. Dominant-negative mutants of a platelet-derived growth factor gene. *Genes Dev* 1990;4:2333–2341. [PubMed: 2279701]
54. Shamah SM, Stiles CD, Guha A. Dominant-negative mutants of platelet-derived growth factor revert the transformed phenotype of human astrocytoma cells. *Mol Cell Biol* 1993;13:7203–7212. [PubMed: 8246942]
55. Hunter GK, Goldberg HA. Nucleation of hydroxyapatite by bone sialoprotein. *Proc Natl Acad Sci (USA)* 1993;90:8562–8565. [PubMed: 8397409]
56. Hunter GK, Hauschka PV, Poole AR, Rosenberg LC, Goldberg HA. Nucleation and inhibition of hydroxyapatite formation by mineralized tissue proteins. *Biochem J* 1996;317:59–64. [PubMed: 8694787]
57. Bronckers AL, Price PA, Schrijvers A, Bervoets TJ, Karsenty G. Studies of osteocalcin function in dentin formation in rodent teeth. *Eur J Oral Sci* 1998;106:795–807. [PubMed: 9672102]

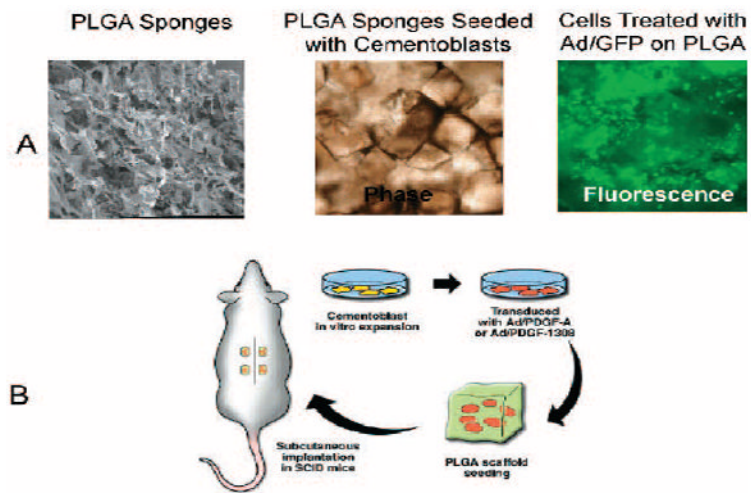


**Figure 1.** Cementum engineering in three-dimensional polymer scaffolds. **A)** Images depict microscopic structure of PLGA scaffold and OCCM cells seeded into the scaffold. The PLGA scaffold exhibits open-pore structures allowing cell penetration and attachment. A representative phase contrast image depicts the PLGA seeded with OCCM transduced with Ad/GFP 48 hours after transduction. The fluorescent image shows the corresponding OCCM cells expressing green fluorescent protein in the scaffold. **B)** Diagram depicts OCCM transduced with adenovirus encoding PDGF-A, PDGF-1308, green fluorescent protein, or NT 24 hours after transduction. The transduced cells were seeded into PLGA polymer scaffold and implanted into SCID mice ( $n = 4$  implants/animal).

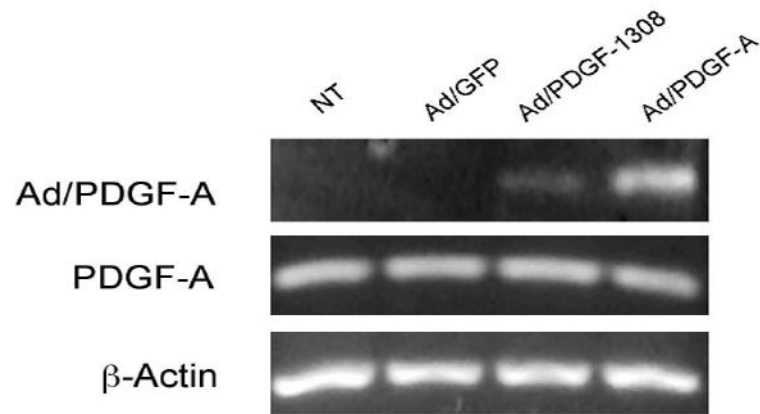


**Figure 2.**

RT-PCR analysis of prolonged PDGF-A, Ad/PDGF-A, and Ad/PDGF-1308 gene expression in vivo. RNA extracted from each implant group was subjected to RT-PCR with primer pairs specifically designed for detecting the expression of PDGF-A and PDGF-1308 transgenes, and endogenous PDGF-A in comparison to  $\beta$ -actin at 6 weeks. PCR products were analyzed on an ethidium bromide-stained gel. Endogenous expression of PDGF-A was detected at similar levels for all treatment groups for up to 6 weeks. Transcripts for Ad/PDGF-A and Ad/PDGF-1308 were noted up to 6 weeks, and were not detected in NT and Ad/GFP-treated implants (n = 3 animals/group).

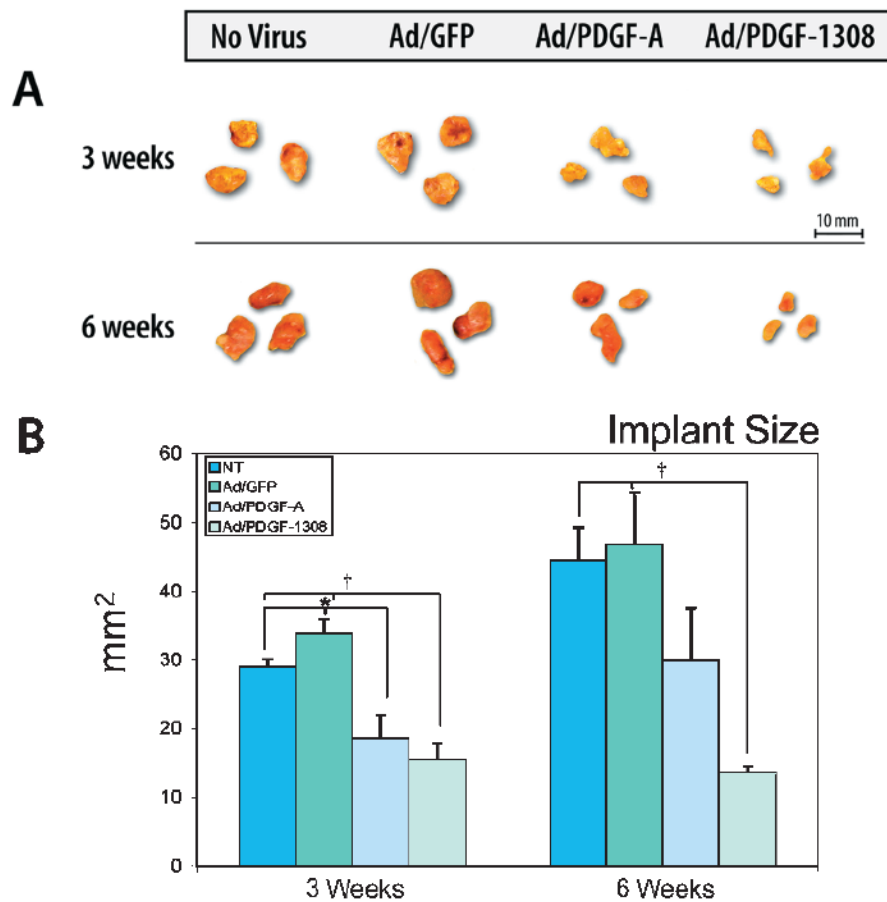


**Figure 3.** Macroscopic appearance and size of retrieved tissue-engineered implants. **A)** Standardized image shows the macroscopic appearance of PLGA-OCCM implants following gene transfer of Ad/GFP, Ad/PDGF-A, Ad/PDGF-1308, or NT at 3 and 6 weeks post-implantation. **B)** Histomorphometric analysis of the peri-implant areas (mm<sup>2</sup>) revealed that Ad/PDGF-A and Ad/PDGF-1308 treated implants were significantly smaller than the NT and Ad/GFP treated groups at 3 weeks (\* $P < 0.05$ ; † $P < 0.01$ ). At 6 weeks, implant size increased for all groups except the Ad/PDGF-1308 group. The Ad/PDGF-1308 treated specimens were significantly smaller when compared with control groups ( $P < 0.01$ ) ( $n = 3$  animals/group).

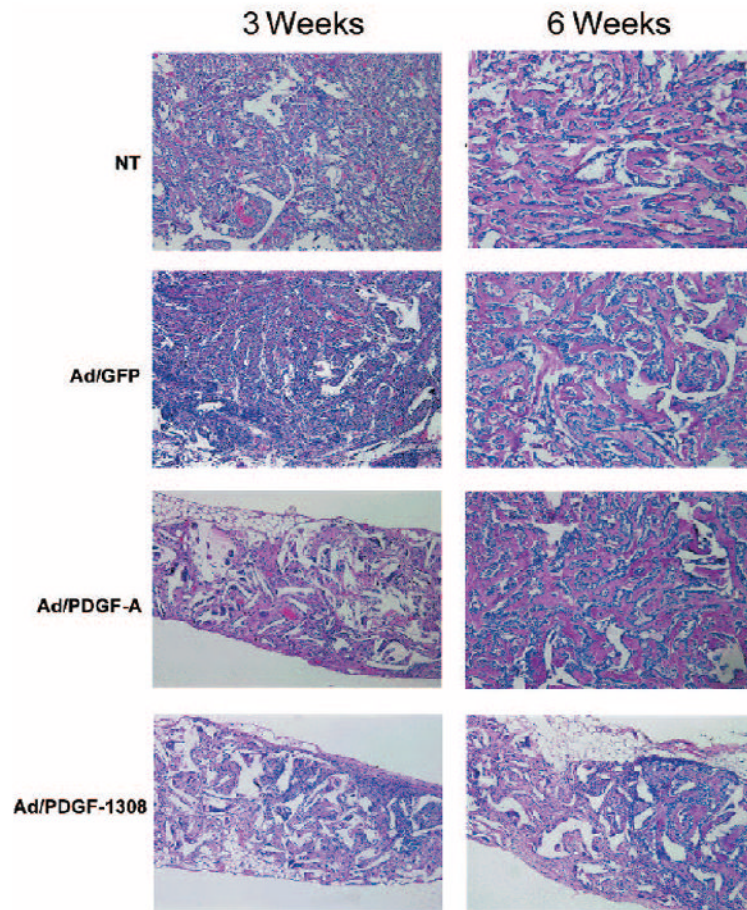


**Figure 4.**

The effect of PDGF-A and PDGF-1308 transgenes on tissue-engineered cementum at 3 and 6 weeks in vivo. Mineralization was minimal to none in the Ad/PDGF-A and Ad/PDGF-1308 treated implants, whereas immature mineral formation was present in the NT and Ad/GFP implants at 3 weeks (left panels). Mineral formed was laced-like, with no hematopoietic or fatty tissue. At 6 weeks, mineral formation progressed in all groups, except the Ad/PDGF-1308 specimens, where minimal mineral formation was noted (right panels). (H&E; original magnification  $\times 100$ ;  $n = 3$  animals/group).



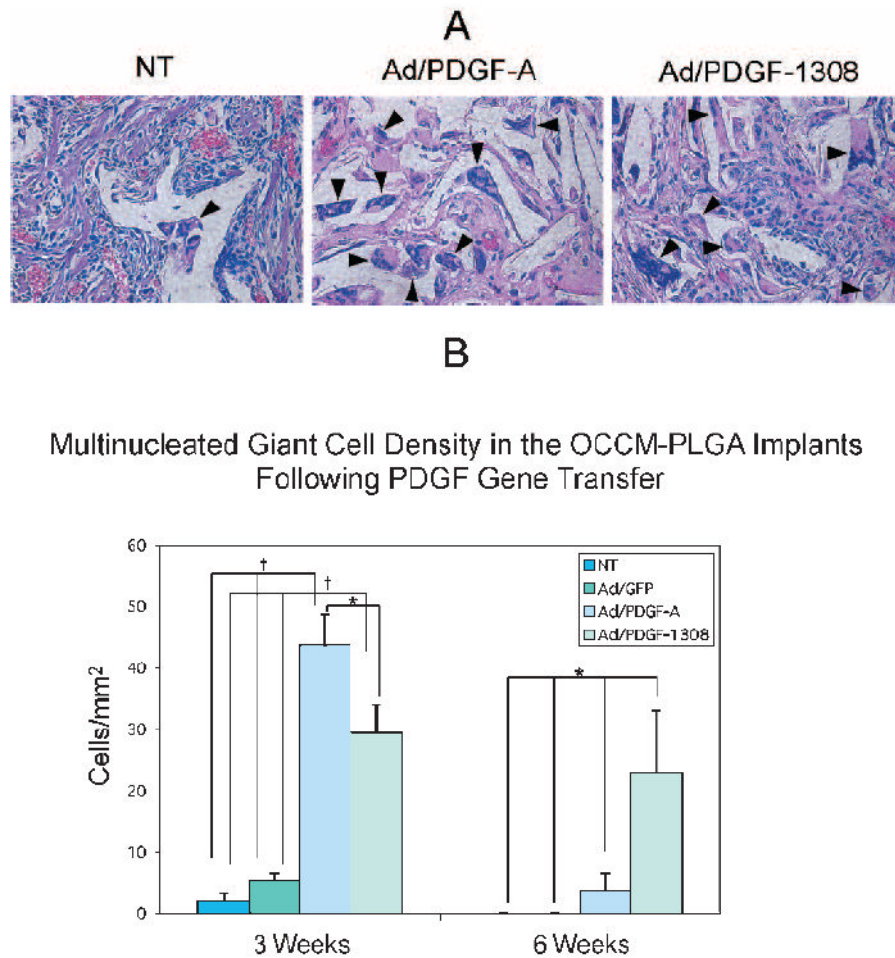


**Figure 5.**

**A)** Images depict infiltration of MNGCs in the OCCM-PLGA implants following NT, Ad/PDGF-A, or Ad/PDGF-1308 gene transfer at 3 weeks. Arrow heads indicate MNGCs. MNGC density at 3 and 6 weeks was determined by dividing total cell numbers by total cross-sectional area for each implant. **B)** Cell density analyses revealed that Ad/PDGF-A and Ad/PDGF-1308 treated groups contained significantly higher MNGC density versus both control groups at 3 weeks ( $\dagger P < 0.001$ ), the Ad/PDGF-A treated implants exhibited greater MNGC density compared to the Ad/PDGF-1308 group at 3 weeks ( $*P < 0.05$ ). At 6 weeks, only Ad/PDGF-1308 treated implants contained significantly higher cell density compared to NT, Ad/GFP, or Ad/PDGF-A groups ( $*P < 0.05$ ). (H&E; 400 $\times$  magnification).

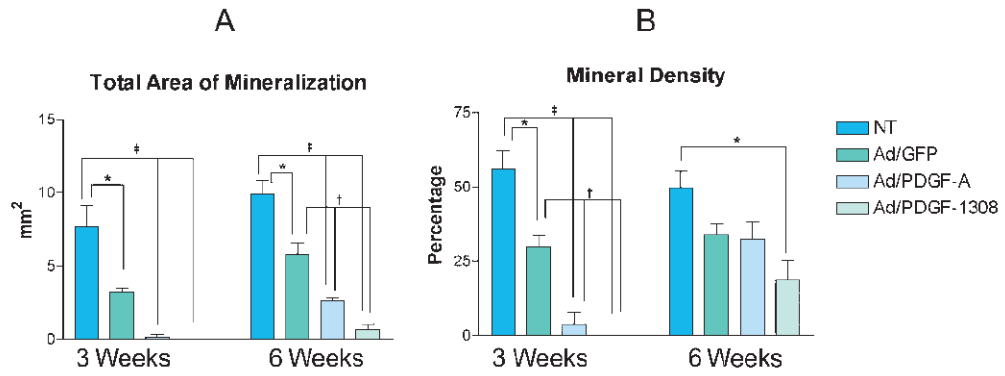


**Figure 6.**

Histomorphometric analysis of mineral neogenesis in OCCM-PLGA implants following gene transfer of Ad/GFP, Ad/PDGF-A, Ad/PDGF-1308, or NT. **A)** Total area of mineral formation and **B)** Percentage of mineral density at 3 and 6 weeks measured by computer-assisted image analysis. The percentage of mineral density equals the total area of mineral formation divided by total area of implant. The data represent mean and standard error of mean for each treatment group. Significantly less mineralization was seen in the Ad/GFP, Ad/PDGF-A, or Ad/PDGF-1308 groups compared to NT at 3 and 6 weeks (\* $P < 0.05$ , † $P < 0.01$ , ‡ $P < 0.001$ ). Percentage of mineral density was significantly less in the Ad/PDGF-A and Ad/PDGF-1308 groups as compared to the NT or Ad/GFP treated groups at 3 weeks. However, mineral density of the Ad/PDGF-A treated groups was comparable to that of the control groups at 6 weeks, while the Ad/PDGF-1308 group remained significantly less versus NT group ( $n = 3$  animals/group).

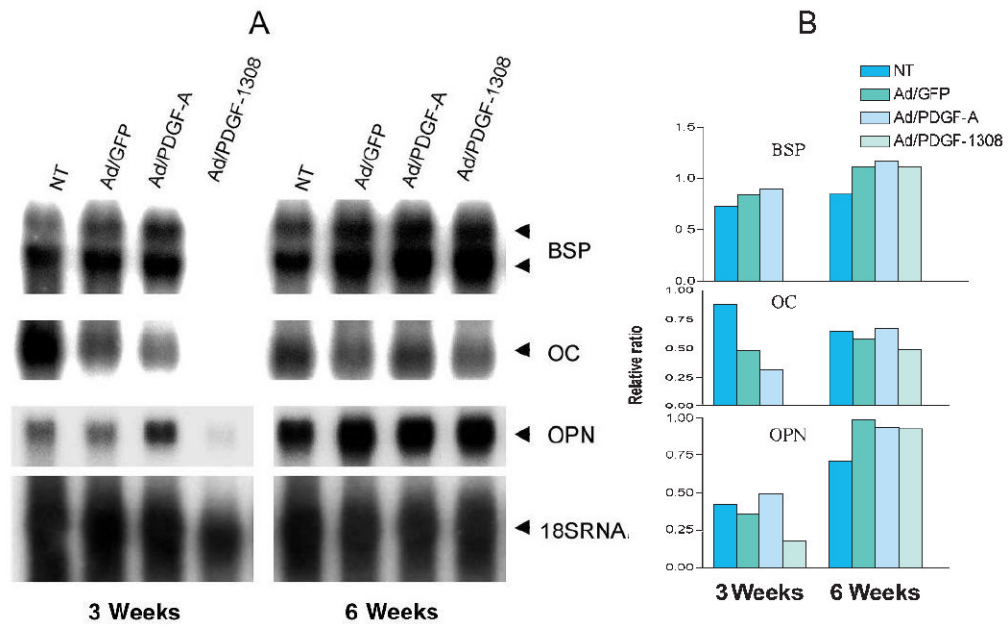


**Figure 7.**

Regulation of mineral-associated genes following PDGF gene transfer in vivo using Northern blot analysis. **A)** Total RNA extracted from NT, Ad/GFP, Ad/PDGF-A, or Ad/PDGF-1308 treated implants at 3 and 6 weeks were harvested and hybridized with  $^{32}\text{P}$ -labeled cDNA probes derived from genes related to mineral formation including bone sialoprotein (BSP), osteocalcin (OC), and osteopontin (OPN). **B)** The relative ratio of BSP, OC, and OPN gene expression was normalized with 18S RNA at 3 and 6 weeks post-implantation using NIH image analysis software. OPN was upregulated in Ad/PDGF-A treated implants, whereas OC was downregulated at 3 weeks. In contrast, BSP, OC, and OPN were downregulated in the Ad/PDGF-1308 treated implants. By 6 weeks, gene expression of BSP, OC, and OPN was similar following gene transfer of Ad/GFP, Ad/PDGF-A, Ad/PDGF-1308, or NT.